Atmos. Chem. Phys., 9, 7053–7066, 2009
www.atmos-chem-phys.net/9/7053/2009/

Atmospheric Chemistry and Physics

Cloud condensation nuclei measurements in the marine boundary layer of the eastern Mediterranean: CCN closure and droplet growth kinetics

A. Bougiatioti[1], **C. Fountoukis**[3,4], **N. Kalivitis**[1], **S. N. Pandis**[4,5], **A. Nenes**[2,3], **and N. Mihalopoulos**[1]

[1]Environmental Chemical Processes Laboratory, Department of Chemistry, University of Crete, Voutes, 71003, Heraklion, Greece
[2]Earth and Atmospheric Sciences, Georgia Institute of Technology, Atlanta, GA, USA
[3]Chemical and Biomolecular Engineering, Georgia Institute of Technology, Atlanta, GA, USA
[4]Institute of Chemical Engineering and High Temperature Chemical Processes (ICE-HT), Foundation for Research and Technology Hellas (FORTH), Patras, 26504, Greece
[5]Department of Chemical Engineering, Carnegie Mellon University, Pittsburgh, PA 15213, USA

Received: 10 March 2009 – Published in Atmos. Chem. Phys. Discuss.: 27 April 2009
Revised: 21 August 2009 – Accepted: 31 August 2009 – Published: 24 September 2009

Abstract. Measurements of cloud condensation nuclei (CCN) concentrations (cm^{-3}) between 0.2 and 1.0% supersaturation, aerosol size distribution and chemical composition were performed at a remote marine site in the eastern Mediterranean, from September to October 2007 during the FAME07 campaign. Most of the particles activate at ~0.6% supersaturation, characteristic of the aged nature of the aerosol sampled. Application of Köhler theory, using measurements of bulk composition, size distribution, and assuming that organics are insoluble resulted in agreement between predicted and measured CCN concentrations within 7±11% for all supersaturations, with a tendency for CCN underprediction (16±6%; r^2=0.88) at the lowest supersaturations (0.21%). Including the effects of the water-soluble organic fraction (which represent around 70% of the total organic content) reduces the average underprediction bias at the low supersaturations, resulting in a total closure error of 0.6±6%. Using threshold droplet growth analysis, the growth kinetics of ambient CCN is consistent with NaCl calibration experiments; hence the presence of aged organics does not suppress the rate of water uptake in this environment. The knowledge of the soluble salt fraction is sufficient for the description of the CCN activity in this area.

Correspondence to: N. Mihalopoulos
(mihalo@chemistry.uoc.gr)

1 Introduction

The absorption and scattering of radiation by atmospheric aerosol particles, especially those from anthropogenic activities, is an important component of anthropogenic climate change (IPCC, 2007). Aerosol particles also act as cloud condensation nuclei (CCN) and "indirectly" force climate through modification of cloud radiative properties and precipitation efficiency (Twomey, 1977; Albrect, 1989). Of all components of anthropogenic climate change, the aerosol indirect effect is the most uncertain (IPCC, 2007). Therefore, accurate prediction of the CCN activity of ambient atmospheric aerosol is required for understanding the impacts of aerosol on the Earth's climate.

The main physical-chemical principles involved in the transformation ("activation") of CCN into a cloud droplet involve the effects of curvature and solute on the equilibrium water vapor pressure. The simplest form of this theory, introduced by Köhler in the early 20th century (Köhler 1921, 1936) was initially developed to describe the activation of marine (NaCl) aerosol particles. With appropriate extensions to account for the multicomponent nature of global aerosol, Köhler theory remains the theoretical basis for linking aerosol to CCN activity, as it determines the characteristic (or "critical") level of ambient water vapor supersaturation, S_c, required for particles to activate into cloud droplets. For a given aerosol particle, S_c depends on the particle dry size and chemical composition. For an aerosol size distribution of known chemical composition, the number

concentration of CCN as a function of ambient supersaturation (the "CCN spectrum") can then be computed and used in physically-based parameterizations of cloud droplet activation (e.g. Nenes et al., 2001; Fountoukis and Nenes, 2005; Barahona and Nenes, 2007).

The ultimate test of Köhler theory is a "CCN closure" study, where measured CCN spectra are compared against predictions from measurements of aerosol chemical composition and size distribution. A successful closure study is when these two quantities are comparable within the measurement uncertainties.

CCN closure studies have been underway many years with varying degrees of success. Liu et al. (1996) measured CCN at Chebogue Point in 1993 during the North Atlantic Regional Experiment (NARE) intensive. With a DH Associates static-diffusion cloud chamber operating at 0.4% supersaturation, size distribution from a PMS passive cavity aerosol spectrometer probe and chemical composition from filter samples, closure was achieved for 75% of the time. Covert et al. (1998) measured CCN concentrations with a static-diffusion cloud chamber at 0.5% supersaturation, and aerosol size distributions with a differential mobility particle sizer during the First Aerosol Characterization Experiment at Cape Grim, Tasmania, 1995. On average closure was obtained with a slight tendency for overprediction (20%).

Cantrell et al. (2001) measured CCN at the Kaashidhoo Climate Observatory during the Indian Ocean Experiment (INDOEX, 1999), using an aerosol time-of-flight spectrometer for the chemical composition and four micro-orifice uniform deposit cascade impactors (MOUDIs). Size distributions were measured using a TSI SMPS and CCN spectra were obtained using a CCN Remover (Ji et al., 1998), resulting in closure in 8 out of 10 cases, with discrepancies increasing with organic mass fraction. Roberts et al. (2003) performed CCN measurements during the Cooperative LBA (Large-scale Biosphere-Atmosphere Experiment in Amazonia, 1998) using a static diffusion cloud chamber between 0.15 and 1.5% supersaturation, a scanning mobility particle sizer for size distribution and a multistage cascade impactor for chemical composition, concluding that the CCN activity of aerosol in the LBA strongly depended on the water-soluble fraction. During the ACE-2 campaign, Snider et al. (2003) and Dusek et al. (2003) both performed CCN closure studies. Snider et al. (2003) attained closure for 2 out of 5 study days, unaffected by continental pollution. Dusek et al. (2003) overpredicted CCN on average by 30%, despite neglecting the effect of WSOC constituents on CCN activity.

VanReken et et al. (2003) performed airborne CCN measurements during the Cirrus Regional Study of Tropical Anvils and Cirrus Layers-Florida Area Cirrus Experiment (CRYSTAL-FACE 2002) using two continuous-flow streamwise temperature gradient chambers (Roberts and Nenes, 2005), at 0.2 and 0.85% supersaturations. Closure was achieved within 5% at 0.2% supersaturation and 9% at 0.85% supersaturation. Using similar instrumentation, Rissman et al. (2006) performed an inverse aerosol-CCN closure, during a 2003 DOE-ARM intensive at the Southern Great Plains site (Oklahoma). Optimum closure was obtained when the population of aerosol was treated as an external mixture of particles, with the insoluble constituents preferentially distributed in particles less than 50nm diameter. Broekhuizen et al. (2006) attained closure within 4% (on average), measuring CCN with a continuous thermal-gradient diffusion chamber at 0.58% for 4 days in Toronto, along with a TSI SMPS and an Aerodyne aerosol mass spectrometer for the size-dependent composition.

During the Chemical Emissions, Loss, Transformation and Interactions with Canopies (CELTIC) field program at Duke Forest in North Carolina, Stroud et al. (2006) measured aerosol size-distribution with a TSI SMPS, chemical composition with an AMS and CCN concentrations with a static-diffusion cloud chamber. CCN predictions were within a factor of two of the observations. Ervens et al. (2007) measured the number concentration of CCN at five supersaturations (0.07 to 0.5%) during the International Consortium for Atmospheric Research on Transport and Transformation (ICARTT) field experiment at Chebogue Point (2004). CCN concentrations were predicted using measured size distributions, a simple aerosol model to derive the solute-to-water mole ratio, and the diameter growth factor or the optical growth factor. The mean error ranged from an overestimate of $\leq$5% at high supersaturation to a factor of 2.4 at low supersaturation. During the same campaign (ICARTT 2004), Medina et al. (2007) measured CCN at the UNH-AIRMAP Thompson Farms site, using a DMT streamwise thermal-gradient CCN counter (Roberts and Nenes, 2005), an AMS for size distribution of chemical composition and a TSI SMPS. Using "simple" Köhler theory and size-averaged chemical composition, CCN were substantially overpredicted (by 35.8$\pm$28.5%) and by introducing size-dependent chemical composition the closure was improved considerably (average error 17.4$\pm$27%).

During the PRIDE-PRD2006 campaign in southeastern China, Rose et al. (2008a) measured and characterized CCN in polluted and biomass burning smoke using a CCN counter and with the use of a constant hygroscopicity parameter of 0.3 deviation between predicted and measured concentrations were on average less than 20%. With variable κ values the relative deviations were on average less than 10%. Gunthe et al. (2009) performed CCN measurements during the AMAZE-08 campaign in central Amazonia, using a continuous-flow CCN counter (DMT-CCNC) in combination with an aerosol mass spectrometer (AMS) to characterize the CCN efficiency and chemical composition of pristine tropical rainforest aerosols. The study resulted in fair agreement and mean relative deviation between measurement results and measurements, parameterized as a function of the organic and inorganic mass fractions, mostly less than 20%.

During the 2006 Gulf of Mexico Atmospheric Composition and Climate Study (GoMACCS), Lance et al. (2009)

used airborne CCN measurements in the highly variable environment of Houston, and attempted CCN closure using a number of compositional assumptions. Assuming the aerosol is internally mixed, CCN were overpredicted by 3% to 36%; for cases where large overprediction was seen, considering external mixing accounted for much of the bias. Organic compounds were not seen to substantially affect CCN activation kinetics.

Murphy et al. (2008) performed the first joint shipboard – airborne study, calculating CCN concentrations at supersaturations ranging from 0.1 to 0.33%. Assuming an internal mixture and using bulk composition, CCN were overpredicted on average by 23±6%; using size-resolved composition reduces error to 16±6%. Important delays in the CCN activation kinetics were observed for particles inside the ship plume, while background marine aerosol activated as quickly as calibration aerosol. Sorooshian et al. (2008) performed an extensive airborne characterization of aerosol downwind of a massive bovine source in the San Joaquin Valley (California). They found that CCN exhibited activation kinetics delays, the extent of which was correlated with organic oxidation state and mass fraction (aerosol with large amounts of hydrophobic organics tend to exhibit retardations in CCN activation kinetics).

The aforementioned studies give a representative but by no means complete subset of the published CCN closure literature; all point out that in Köhler theory sufficiently describes the activation of ambient aerosol, provided that the chemical composition, aerosol size distribution and mixing state are well constrainted. CCN prediction error most often arises from sampling or instrumentation limitations, especially when determining the aerosol chemical composition. The latter is quite important if the aerosol is externally mixed, or contains a large fraction of organic compounds. However, the treatment of organics in Köhler theory remains challenging and may explain some of the observed discrepancies in previous studies. A comprehensive application of Köhler theory, that accounts for the effects of the water-soluble organic carbon (WSOC) fraction of the aerosol is challenging for a number of reasons. WSOC can act as a surfactant, lowering droplet surface tension (Facchini et al.,1999; Decesari et al., 2003) and may also contribute solute (Shulman et al., 1996), although the presence of soluble inorganic salts can diminish its importance (e.g. Ervens et al., 2007). Salma et al. (2006) found that humic-like substances (HULIS) make up to 54% of this WSOC, and these substances are known to lower the surface tension of solution droplets (Ziese et al., 2008). Dinar et al. (2006) reported reductions in surface tension by 25–45% compared to the surface tension of water, with the measured surface tensions depending on the concentration and the age of the solution (Ziese et al., 2008). The insoluble fraction of organics may also affect the uptake rate of water (e.g. Asa-Awuku et al., 2009) with important implications for cloud droplet number (e.g. Nenes et al., 2002). Since each of these effects alone can either enhance or diminish the CCN activity and droplet number in ambient clouds, the interpretation of the role of organics on CCN activation may be quite complex, and requires observational constraints to express their combined importance.

In the present paper, we report the CCN concentrations and the activation characteristics of atmospheric aerosols in a diversity of air masses sampled at an Eastern Mediterranean ground site during the Finokalia Aerosol Measurement Experiment-2007 (FAME-07) campaign. The present study is the first to report data of CCN measurements in the area, and complements existing studies on the aerosol characteristics in this climatically sensitive area of the globe (Lelieveld et al., 2002; Vrekoussis et al., 2005). In the following sections, CCN closure studies are carried out, with the goal of testing the applicability of "simple" Köhler theory for the prediction of CCN concentrations in a remote area with aged aerosol. The contribution of the aerosol organic fraction to CCN activity is also assessed, as well as their potential impact on droplet activation kinetics.

2 Observational data set

2.1 Measurement site

The Finokalia station (35°32′ N, 25°67′ E; http://finokalia.chemistry.uoc.gr) is a remote marine background site (50 m from the shore and 230 m above sea level) established and operated by the University of Crete. A detailed description of the site and prevailing meteorology can be found in Mihalopoulos et al. (1997) and Sciare et al. (2003). Finokalia is located at a unique "crossroad" of aged aerosol types, which can originate from the marine boundary layer, Saharan desert, European subcontinent, and, biomass burning events during the summer period. The measurements presented in this study were obtained from mid-June to mid-October 2007, during the FAME-07 campaign, focused on understanding the properties of regional aged aerosol and their effects on regional climate. Analysis of HYSPLIT backtrajectories (www.arl.noaa.gov/ready/hysplit4.html) are then used to correlate measured aerosol properties with air mass origin. Throughout the campaign, both "polluted" air masses from Europe, the former Soviet Union and Asia Minor (Fig. 1a, b) and "cleaner" air masses from the Mediterranean and North Africa (Fig. 1c, d) were sampled.

2.2 Instrumentation setup

The instrumentation setup consisted of a Droplet Measurement Technologies (DMT) streamwise thermal-gradient CCN counter (Roberts and Nenes, 2005), a scanning mobility particle sizer (SMPS TSI 3080; composed of a TSI 3010 condensation particle counter and a TSI 3081L differential mobility analyzer), used to measure the dry aerosol size distribution. The bulk (PM_1, $PM_{1.3}$, $PM_{1.3-10}$ and PM_{10}) aerosol chemical composition was concurrently measured,

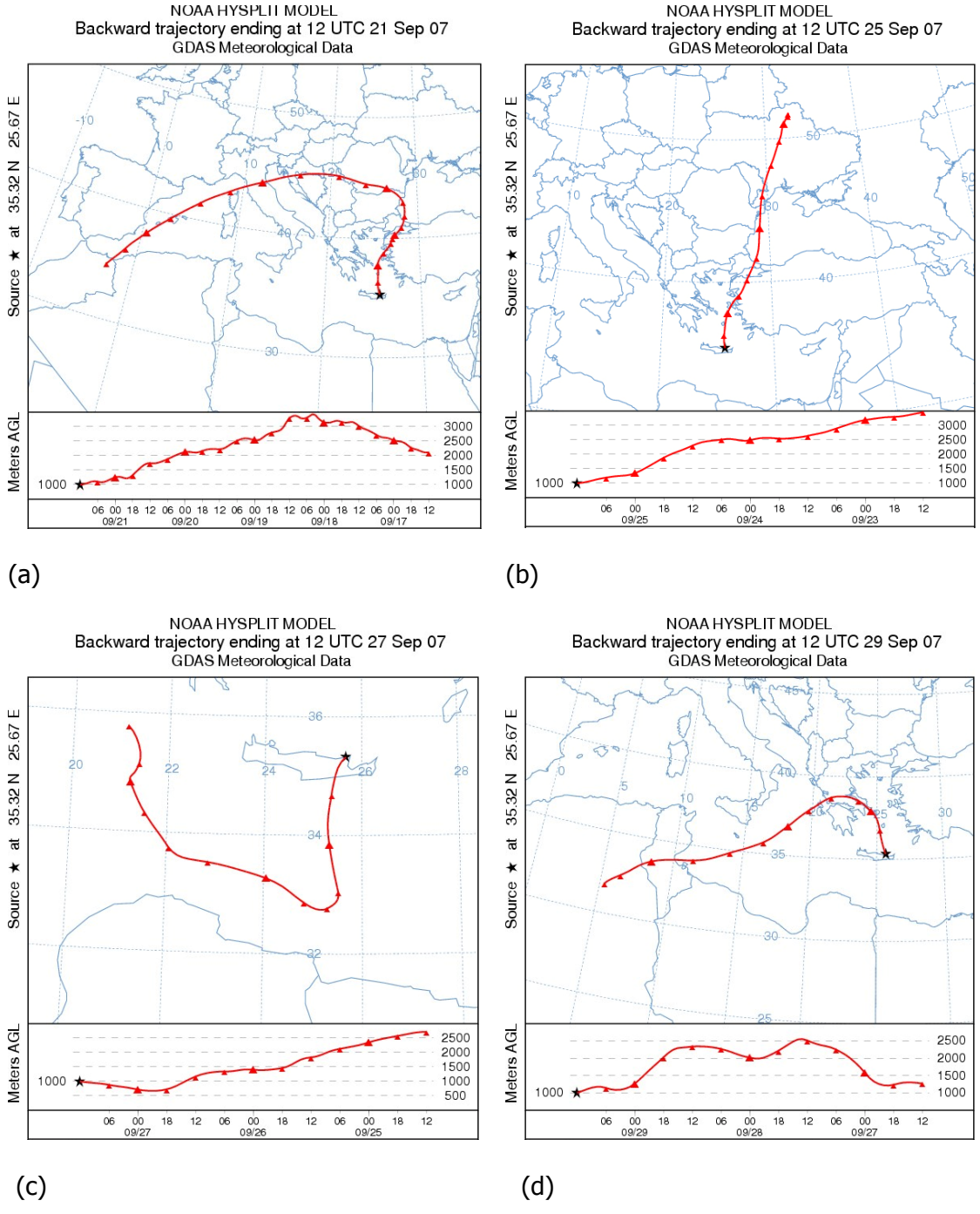

Fig. 1. Maps indicating the location of the sampling site and three-day HYSPLIT back trajectories for characteristic types of air masses sampled during FAME-07: **(a)** 20 September 2007 (Period "A"), **(b)** 22 September 2007 (Period "B"), **(c)** 27 September 2007 (Period "C"), and **(d)** 29 September 2007 (Period "D").

using 4-h filter samples that were continuously collected during the campaign. Auxiliary chemical measurements (O_3, NO_x, CO, BC, Rn-222) and meteorological parameters (wind speed and direction, pressure, temperature, relative humidity) were also continuously monitored.

2.3 CCN measurements

The DMT CCN counter (Roberts and Nenes, 2005; Lance et al., 2006) is a cylindrical continuous-flow streamwise thermal gradient diffusion chamber. A constant streamwise

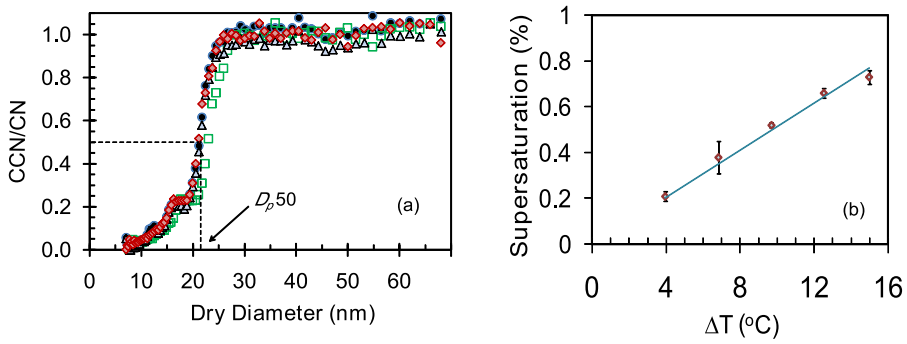

Fig. 2. (a) Activation curves for NaCl calibration aerosol, obtained for a top-bottom column temperature difference, ΔT=15 K. **(b)** Instrument supersaturation versus ΔT.

temperature gradient is applied along the walls of the instrument flow chamber; the higher diffusivity of water vapor, relative to heat, results in supersaturation developing in the flow chamber. Before its introduction into the flow chamber, the sample is split into a "sheath" and an "aerosol" flow. The "sheath" flow is filtered and humidified before its entry in the chamber, whereas the "aerosol" flow is introduced at the centerline of the flow and exposed to a constant supersaturation. The supersaturation is controlled by the chamber flow rate and the streamwise temperature gradient (Roberts and Nenes, 2005). The fraction of particles in the sample with S_c less than the instrument supersaturation activate into cloud droplets, are counted and sized upon exit from the flow chamber in an Optical Particle Counter (OPC) using light from a 658 nm diode laser. A multichannel analyzer classifies the detected droplets into 20 size classes (from 0.75 to 10 μm diameter) and size distribution histograms are reported at 1 Hz frequency. Throughout the campaign, the instrument was operated at a total flow rate of 0.5 L min^{-1}, with a sheath-to-aerosol flow ratio of 10:1, and a top-bottom column difference, ΔT, between 4 and 15 K. Concentrations were measured at each supersaturation for 6 min, yielding a CCN spectrum consisting of 5 different supersaturations every 30 min.

Calibration of the instrument supersaturation was done by determining the minimum diameter, D_p, of classified NaCl aerosol that activates at given chamber flow rate and ΔT. NaCl aerosol was generated by atomizing a sodium chloride aqueous solution (via a collision-type atomizer) and subsequently drying the droplet stream by passing it through two silica-gel diffusional driers (operating at ~5% RH). The resulting polydisperse dry aerosol was then charged using a Kr-85 neutralizer (TSI 3077A), and classified using a TSI 3080 Scanning Mobility Particle Sizer (SMPS) (consisted of a TSI 3010 condensation particle counter and a TSI 3081 differential mobility analyzer, DMA, operating under a sheath-to-aerosol ratio of 10:1). The classified aerosol flow was split and concurrently introduced into the CPC and the CCN instrument; the concentration of total particles (or, condensation nuclei, CN) and CCN were measured, and the activation fraction (CCN/CN) was computed. This process was repeated over many classified particle sizes (between 10 and 460 nm), so that an "activation curve" (i.e. CCN/CN as a function of mobility diameter) was obtained, which exhibits a characteristic sigmoidal shape. The critical supersaturation of the particle with dry diameter, D_{p50}, at which half of the classified aerosol activates (i.e. CCN/CN=0.5) is used to characterize the instrument supersaturation. Köhler theory (Eq. 2) is used to compute S_c from D_{p50}, assuming that the density of NaCl is equal to 2160 kg m^{-3} (CRC, 1993), surface tension of water and a molar mass of 0.058 kg mol^{-1}. The van't Hoff factor, υ_s, was calculated as $\nu\Phi$, where ν=2 are the moles of ions released into solution per mole of NaCl, and, Φ is the osmotic coefficient calculated by application of the Pitzer ion-interaction model (Pitzer and Mayorga, 1973) using interaction parameters provided by Clegg and Brimblecombe (1988). Φ is computed at the concentration corresponding to the CCN critical point (also computed from Köher theory; Padró et al., 2007). For the range of supersaturations considered in the calibrations (0.21 and 0.73%), υ_s ranged between 1.91 and 1.87. This calibration procedure is repeated over a number of ΔT. As dry sodium chloride particles generated from atomization of a solution are usually of cubic shape (Krämer et al., 2000; Mikhailov et al., 2004), a shape factor of 1.08 must be considered in the diameter calculations (Rose et al., 2008b). Figure 2a shows examples of activation curves obtained throughout the campaign (for a flow rate of 0.5 lpm and ΔT=15 K); application of Köher theory to the observed D_p50 yields an instrument supersaturation of 0.73±0.03% (the supersaturation uncertainty is obtained from the observed range in D_p50 in the calibrations). Figure 2b shows supersaturation versus the instrument operating temperature difference, ΔT, with error bars representing the standard deviation between calibrations. The CCN instrument was calibrated numerous times throughout the campaign to characterize the stability of its characteristics. For the lower supersaturations, the relative variability between calibrations did not exceed 1%, whereas for the highest supersaturation the variability was under 3%.

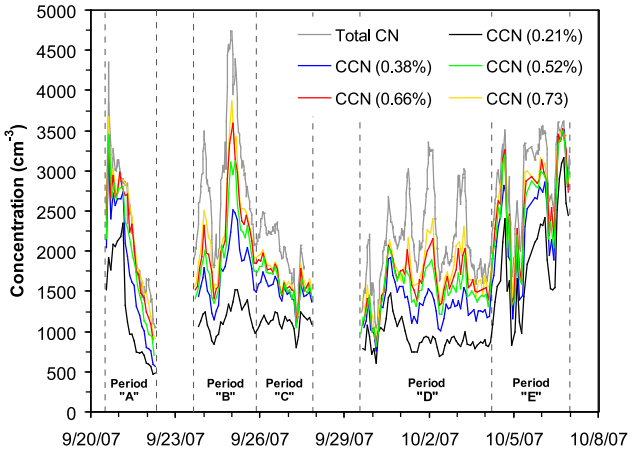

Fig. 3. Time series of the CN and CCN measurements throughout the measurement period.

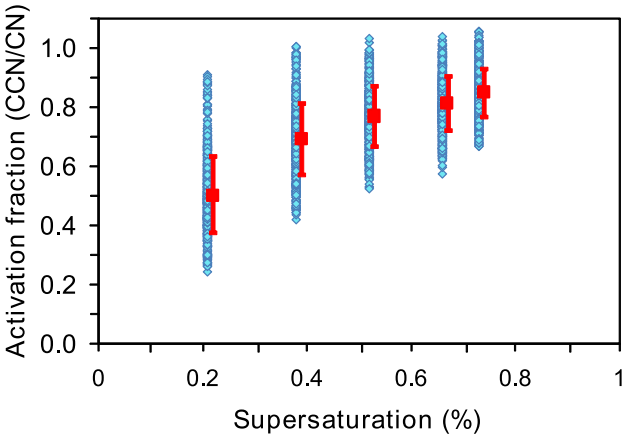

Fig. 4. Measured activation fraction versus supersaturation for the ambient aerosol, with the mean value and standard deviation from mean marked with red.

2.4 Dry size distribution measurements

Prior to introduction into the SMPS, ambient aerosol was dried using two silica gel diffusional dryers, then charged by a Kr-85 neutralizer (TSI 3077A) and introduced into the DMA. The classified aerosol was then introduced into a TSI 3010 condensation particle counter (CPC) for measurements of particle concentration. The particle size distribution was obtained during a scan cycle (3 min) for mobility diameters between 20 and 460 nm. The sample flow rate in the DMA was set to 0.5 L min^{-1} and the sheath-to-aerosol flow ratio was maintained at 10:1.

2.5 Chemical composition

The aerosol chemical composition was determined by analysis of PTFE (PM_{10}, $PM_{1.3}$ and $PM_{1.3-10}$) and quartz (PM_1 and PM_{10}) filter samples (where aerosol was collected over 4 h). PTFE and quartz filters were analyzed for water-soluble ions after extraction with nanopure water. The solutions obtained were analyzed by ion chromatography (IC) for anions (Cl^-, Br^-, NO_3^-, SO_4^{2-}, $C_2O_4^{2-}$) and cations (K^+, Na^+, NH_4^+, Mg^{2+}, Ca^{2+}), using the procedure of Bardouki et al. (2003). Quartz filters were also analyzed for organic and elemental carbon (Carbon Aerosol Analysis Lab Instrument, SUNSET Laboratory Inc.) and for water-soluble organic carbon (TOC-V_{CSH}, Total Organic Carbon Analyzer, SHIMATZU).

3 Results and discussion

3.1 CCN measurements

The time series of the total CN obtained from integration of the SMPS size distributions, and CCN measurements are shown in Fig. 3. The CCN generally correlate well with CN, with CCN concentrations increasing, as expected, with supersaturation. Throughout the measurement period, CCN concentrations at each supersaturation level varied by up to a factor of 3. The measured CCN concentrations at 0.51, 0.66 and 0.73% supersaturation were often very similar. The high activation fractions at these supersaturations, and the small change between 0.5% and 0.75% therefore suggests that most particles are activated at ∼0.6% supersaturation. The latter can be also derived from Fig. 4, where the activation fraction of the measured CCN versus total CN approaches unity at high supersaturations. This behavior is consistent with sampling aged aerosol, where particles are large in size and contain significant amounts of soluble material.

The CCN concentration time series can be divided in five periods, based on the origin of the air masses sampled (Fig. 3). Period "A" represents the high CCN concentrations from air masses coming from the Balkans. The highest concentrations were observed on the 25 September, during Period "B", when air masses originated from NE Europe. Period "C" was characterized by a decrease in CCN concentrations, consistent with marine aerosol that did not have contact with land during the three days prior to its arrival at Crete. As the wind direction shifted later on to westerly (Period "D"), the air originated from North Africa then briefly passed over the Balkans before arriving at Crete. The airmass is thus largely marine but with elevated CCN concentrations associated with the continental influence. In the beginning of October (Period "E"), CCN concentrations were high (especially toward the end of the measurement campaign), as air masses were coming from Asia Minor and NE Europe. The lowest CCN concentrations were observed on the 22 September, after Period "A", as air originated from high in the free troposphere and descended into the marine boundary layer without passing near major aerosol sources. These results are summarized in Fig. 5a, showing the CCN concentrations grouped by prevailing wind direction.

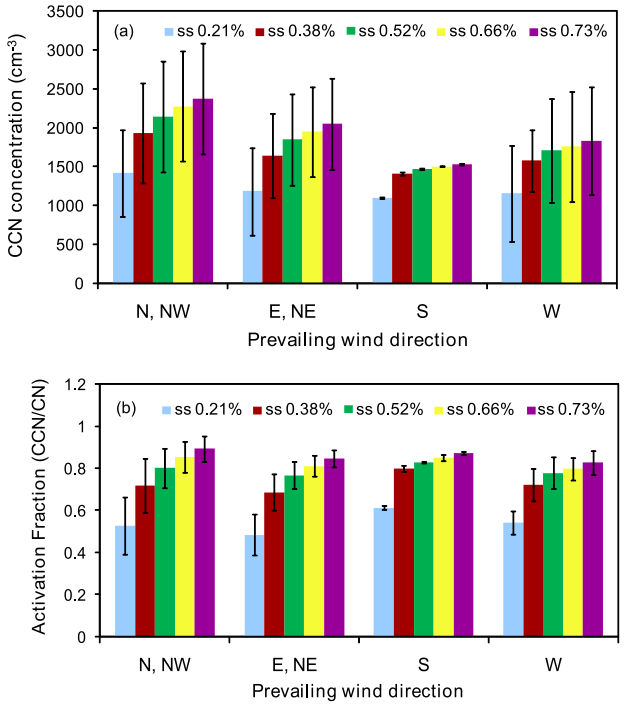

Fig. 5. (a) CCN average concentrations and corresponding standard deviations, and, **(b)** activation fraction and corresponding standard deviation for each prevailing wind direction.

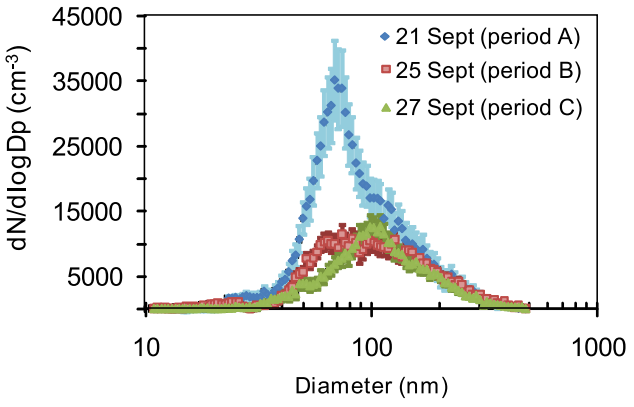

Fig. 6. Daily average aerosol size distributions, characteristic of the air masses sampled.

The large scatter in measured activation fraction at each supersaturation (Fig. 4) is partially due to the air mass origin. This is shown clearly in Fig. 5b, which presents the measured CCN/CN separately for each wind direction. For the low supersaturations (0.21, 0.38%), CCN/CN is larger when the air masses are "cleaner" i.e. when they are originated from the South (Fig. 5b). For the high supersaturations the ratio remains more or less constant (and close to unity, since most of the aerosol activates), regardless of the air mass origin. The slopes of all of the CCN spectra (excluding the one from the South) are similar, consistent with their continental origin.

3.2 Aerosol mass and composition measurements

The distinction between "polluted" (Fig. 1a, b) and "cleaner" (Fig. 1c, d) air masses suggested from the back trajectories is reflected in the size distribution measurements (Fig. 6). Aerosol concentrations in air masses originating from central Europe (21 September) were significantly higher (t-test, 99% confidence level), exhibiting a maxima in the range of 60 nm. The size distributions for air masses originating from northeastern Europe (25 September) and from the South (27 September) are rather similar, with a maxima in the range of 100 nm. The main difference between the two is the presence of a somewhat elevated fraction of particles with sizes below 100 nm for 25 September consistent with the continental origin of the air masses. The corresponding average number concentrations for the aforementioned dates were 7804±929, 4119±386 and 3463±373 cm^{-3}, respectively. For particles smaller than 40 nm, the values were 897±178, 467±71 and 289±81 cm^{-3}, respectively.

The average particulate matter concentration during the measurement period was of 15.82±8.3 $\mu g\,m^{-3}$, with the PM_1 fraction accounting for 60.5±6.5% of the total mass. Ammonium sulfate accounted for 62.4±12% of the total inorganic mass fraction, with 80±10% of the total sulfate being in the fine mode. The remaining 19.6±10% of the inorganic mass consists mostly of Ca^{2+}, and on occasion, small amounts of Cl^- and NO_3^-. From the organic carbon analysis, the fine mode (PM_1) represented 74.8±12.3% of the total organic carbon concentration, varying from 0.6 to 4.1 $\mu g\,m^{-3}$. The similar PM_1/PM_{10} ratios for organics and sulfate are consistent with an internally mixed aerosol, at least for sizes above 1 μm. The WSOC analysis showed that 70% of the organic carbon was water-soluble, with this ratio remaining more or less constant throughout the whole measurement period. This ratio though high, is consistent with the aged nature of the aerosol (Jaffrezo et al., 2005 and references within). Finally, Fig. 7 shows the time series of the particulate organic matter and the ammonium sulfate loadings ($\mu g\,m^{-3}$) resulting from the compositional analysis, with an average of 8.6 $\mu g\,m^{-3}$ and 6.4 $\mu g\,m^{-3}$, respectively.

The aerosol hygroscopicity parameter, κ, is also calculated for all the data considered here. κ is a parameterization of the solute term in Köhler theory, and is used to compared the hygroscopicity of aerosol with different composition (Petters and Kreidenweis, 2007). κ is calculated as the volume-fraction weighted average κ of the aerosol constituents ($\kappa=\kappa_s\varepsilon_s+\kappa_o\varepsilon_o$). κ_s=0.6 applies to ammonium sulfate (Petters and Kreidenweis, 2007), κ_o=0.16 is the organic hygroscopicity parameter, and ε_s, ε_o are the volume fractions of each constituent (Sect. 3.3). κ for all the data in this study is presented in Fig. 7c. Throughout the

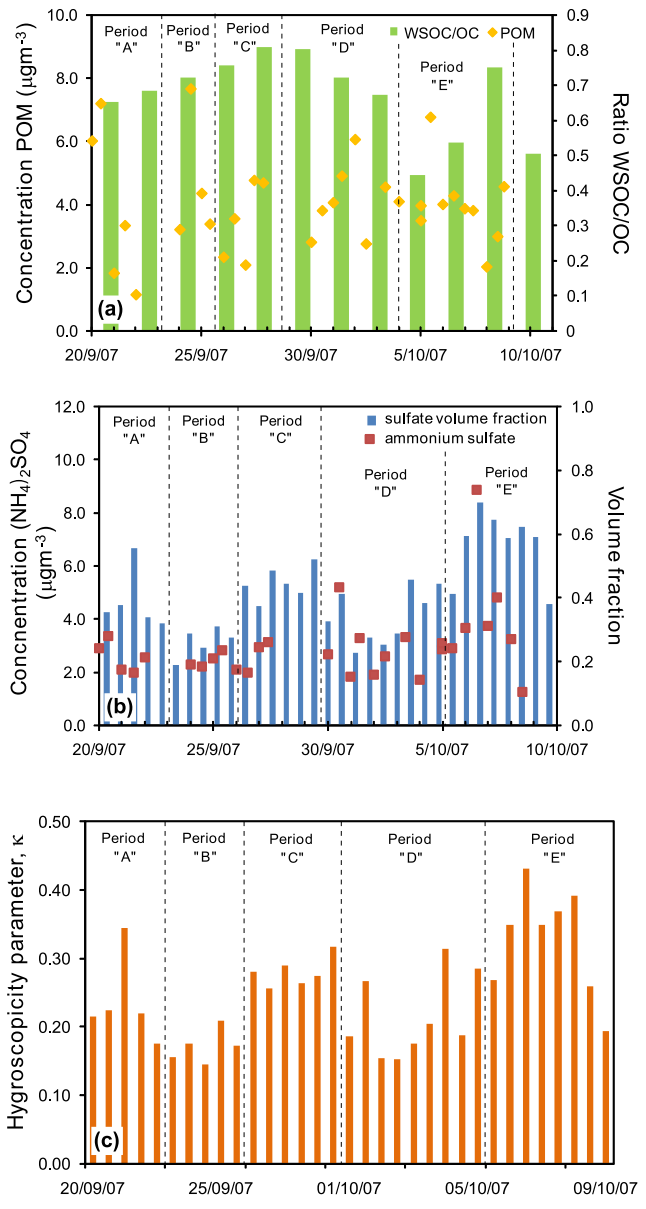

Fig. 7. Time series of the **(a)** particulate organic matter (PM_{10}) and WSOC/OC ratio, **(b)** ammonium sulfate concentration (PM_{10}) and the sulfate volume fraction and **(c)** hygroscopicity parameter κ.

measurement period the aerosol exhibited values between low hygroscopicity ($\kappa \approx 0.1-0.2$) and medium hygroscopicity ($\kappa \approx 0.2-0.5$), with a resulting average value of 0.24, close to the proposed global average of 0.3 (Andreae and Rosenfeld; 2008 and Pöschl et al., 2009). Given that κ is strongly influenced by the amount of sulfate in the aerosol, it is correlated with the sulfate volume fraction Fig. 7b).

3.3 CCN closure

Before each closure calculation, the transients in the CCN instrument operation were screened to minimize observational biases. Each 6-min supersaturation segment was examined for (a) minimal fluctuations in the flow chamber temperature gradient, and, (b) stability of the flows. Fluctuations in temperature, if small enough, have a minimal impact on instrument supersaturation and closure (Ervens et al., 2007). If both criteria were satisfied, then the CCN concentrations were averaged over the last 2–3 min of each supersaturation; closure calculations were done using SMPS size distributions for scans overlapping with the CCN measurements. The chemical composition for computing CCN properties was obtained from the analysis of the corresponding 4-h filters.

Most of the inorganic soluble fraction was ammonium sulfate ($greqs_{NH4}/greqs_{SO4}$=0.93, "greqs" being the gram equivalents of each ionic species); other inorganic components are neglected, their concentration in moles was low throughout the measurement period (a sensitivity study in Sect. 3.4 however addresses their potential impact on the closure). Thus, we assume the aerosol to be composed of a mixture of $(NH_4)_2SO_4$ and organics, and, the ammonium sulfate volume fraction, ε_s can be calculated as

$$\varepsilon_s = \frac{\frac{m_s}{\rho_s}}{\frac{m_s}{\rho_s} + \frac{m_i}{\rho_i}} \quad (1)$$

where ρ_i, ρ_s is the density of the organic (1500 kg m^{-3}; Kostenidou et al., 2007) and $(NH_4)_2SO_4$ (1760 kg m^{-3}), respectively, and m_i, m_s are the mass loadings of organic and $(NH_4)_2SO_4$, respectively. For the measurement period, the volume fraction of ammonium sulfate had a mean value of 0.378±0.144. These values are consistent with long-term measurements in this site, where ammonium sulfate accounts for 46±10% of the total aerosol mass (the largest part of which, 84±8%, being in the fine mode), and remains fairly constant throughout the year (Koulouri et al., 2008).

Based on the composition computed from Eq. (1), the critical supersaturation, Sc for each particle size d, is calculated from Köhler theory (e.g. Seinfeld and Pandis, 1998),

$$Sc = \left[\frac{256}{27}\left(\frac{M_w\sigma}{RT\rho_w}\right)^3\left(\frac{\rho_w}{M_w}\right)\left(\frac{M_s}{\rho_s}\varepsilon_s\upsilon_s + \frac{M_o}{\rho_o}\varepsilon_o\upsilon_o\right)^{-1} d^{-3}\right]^{1/2} \quad (2)$$

where R is the universal gas constant, T is the ambient temperature, σ is the surface tension of the CCN at the point of activation (assumed to be equal to that of water), M_s is the molar mass of the solute and M_w, ρ_w are the molar mass and density of water, respectively, computed at the average temperature of the CCN column. As done for NaCl calibration aerosol, the effective van't Hoff factor of the sulfate, υ_s, is computed as $\upsilon\Phi$, where υ=3 for $(NH_4)_2SO_4$, and Φ is computed from the Pitzer activity model (Pitzer, 1973), for

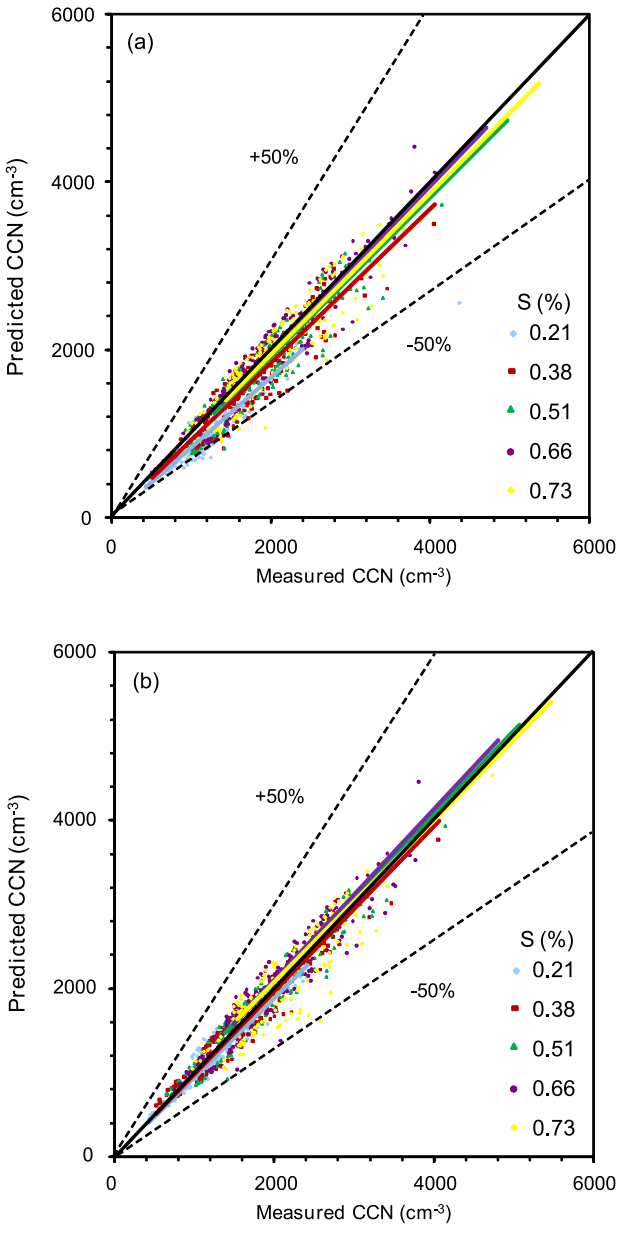

Fig. 8. Calculated versus measured CCN concentrations; **(a)** without and **(b)** with considering 70% of organics to be water-soluble.

the solute concentration at the critical point. M_o, ρ_o, ε_o, v_o in Eq. (2) are the molar mass, density, volume fraction and effective van't Hoff factor of the water-soluble organic fraction, respectively.

Predicting CCN concentrations for a closure study entails computing S_c for each aerosol size class in the measured size distributions, using the measured composition (Eq. 1). CCN are then considered those particles for which S_c is less or equal to the instrument supersaturation during the time of the measurement. In applying Eq. (2), two cases are investigated: (a) assuming that the organic fraction is insoluble, i.e. ε_o=0, and, (b) that 70% of the organics are water-soluble (as suggested by a carbon mass balance of extracted filters), i.e. ε_o=0.7(1-ε_s), where (1-ε_s) is the volume fraction of the organics in the particles, and v_o=1. In reality, 70% organic solubility is an upper limit for the organic water-soluble fraction, since the amount of water mass available in recently activated CCN is usually much less than that used for WSOC filter extraction. In application of Eq. (2), we use M_o∼200, consistent with values inferred from Köhler theory analysis of water-soluble organic samples collected from a variety of sources (Asa-Awuku et al., 2007, 2008, 2009; Englehart et al., 2008). For WSOC a density of ρ_o=1500 kg m^{-3} (Kostenidou et al., 2007; Engelhart et al., 2008) was also used and assumed to be equal to the organic. As the oxygen-to-carbon ratio in the organic and water-soluble organic carbon is somewhat uncertain, the fraction of the water soluble to organic matter (WSOM/OM) is also uncertain, albeit high. Therefore, the density of the OC is close to that of WSOC and is treated as equal in the CCN concentration calculations; a closure sensitivity analysis of the density to the closure is performed (Sect. 3.4). The density is varied based on measurements of ambient data; a "basecase" of 1500 kg m^3 is taken, with a lower limit of 1400 kg m^3 (Cross et al., 2006; Turšiè et al., 2006; Hallquist et al., 2009) and an upper limit of 1600 kg m^3 (Stein et al., 1994; McMurry et al., 2002). The value of organic density, molar mass and van't Hoff factor used here yields a hygroscopicity parameter for the organic fraction $\kappa_{\text{org}} = \left(\frac{M_w}{\rho_w}\right)\left(\frac{\rho_o}{M_o v_o}\right) \approx 0.158$, which is within the range of hygroscopicities reported for highly aged (oxidized) organic material (Petters and Kreidenweis, 2007).

Figure 8a shows the predicted against measured CCN for the whole measurement period, assuming that the organics are insoluble. On average, the closure is achieved to within 7±11%. For the lowest supersaturation (0.21%) there is an underprediction bias which is not seen at higher supersaturations (Table 1). The underprediction bias at low supersaturation could result, in part, from neglecting the impact of soluble organics in the calculations. Indeed, the closure error (−0.6±9% from −7±11%) and scatter (R^2=0.92 from R^2=0.90) are markedly reduced when the average organic water-soluble fraction is considered in the CCN calculations. The underprediction bias at low supersaturations is also substantially reduced to 5% (Fig. 8b). Using the time-dependant WSOC/OC ratio does not affect the closure, as it varies CCN predictions by +1.03% (not shown).

Variations in size-dependant composition could also contribute to the slight underprediction bias remaining after inclusion of water-soluble organic effects; a 5–10% sulfate fraction variation in the lower critical-supersaturation particles (corresponding to those with ∼100 nm diameter) would account for this bias, and possibly, scatter (Sect. 3.4). Long-term size-resolved chemical composition observations at the site (collected with a 12-stage Small-Deposit-area-low-

Table 1. Regression statistics for the CCN closure.

Supersaturation (%) (data points)	WSOC/OC=0		WSOC/OC=0.7	
	$\frac{CCN_{\text{predicted}}}{CCN_{\text{observed}}}$	R^2	$\frac{CCN_{\text{predicted}}}{CCN_{\text{observed}}}$	R^2
0.21 (261)	0.84	0.88	0.95	0.92
0.38 (265)	0.92	0.89	0.98	0.93
0.52 (265)	0.95	0.90	0.99	0.93
0.66 (265)	0.99	0.92	1.01	0.92
0.73 (266)	0.96	0.91	0.98	0.90

volume-Impactor; Maenhaut et al., 1996) reveal similar size-resolved composition variability, with the concentrations of the major aerosol components (OC, NH_4^+, SO_4^{2-}) being fairly constant in every stage, regardless of season. The maximum concentrations are observed at the sizes with geometric diameter of 0.346 μm (i.e. 240 nm mobility diameter), exhibiting a variability of concentrations on the order of 5–10% (not shown). This, together with the fairly constant single lognormal mode spanning the 60–400 nm size range in each airmass period (Fig. 6) hints that the variation in sulfate fraction may occur, but it is likely minor, and at levels consistent with the CCN prediction bias and scatter.

Our results are consistent with other published CCN closure studies, in that the largest prediction biases tend to be seen at the lowest supersaturarion (Chang et al., 2007; Gunthe et al., 2009; Medina et al., 2007). Considerably lower closure error is seen compared to studies carried out close to heterogeneous aerosol sources (e.g. Medina et al., 2007; Stroud et al., 2007; Lance et al., 2009), which show as much as twofold overprediction in CCN concentrations.

3.4 Sensitivity of CCN closure to aerosol parameters

In this section, the sensitivity of CCN closure to aerosol properties assumed (i.e. organics density, and aerosol compositional measurement uncertainties) as well as the uncertainty in the gravimetric measurements (i.e. uncertainty in mass, volume fraction) is conducted. Generally it is observed that a 10% increase in the organic density improves the closure (+2%), and so does a 7% increase of the ammonium sulfate mass, which is even more apparent for the lowest supersaturation (+5%). The respective closure errors ($CCN_{\text{predicted}} - CCN_{\text{measured}}/CCN_{\text{measured}}$) between the original calculation and the increased organic density and ammonium sulfate mass are -2.9 ± 15 and -3.4 ± 14%. Likewise, a 10% decrease in the organic density has a similar effect in the closure (-2%) as a 7% decrease of the ammonium sulfate mass, which is also more apparent for the lowest supersaturation. Overall, a ±10% change in the density of the organics results or a ±7% change in the ammonium sulfate mass, obtained from the experimental analysis, does not substantially impact closure.

3.5 Droplet activation kinetics

Even though the soluble fraction (organic and inorganic) controls CCN activity, the insoluble organic fraction can also affect droplet formation by changing the uptake rate of water vapor onto growing droplets (e.g. Asa-Awuku, 2009). The OPC of the CCN counter provides information about the size of activated droplets as they exit the growth chamber. This can be used to assess the impact of the organics on the uptake rate of water vapor onto the growing CCN, using a method called "Threshold Droplet Growth Analysis" (TDGA). For this, droplet sizes from activated ambient CCN are compared to those of pure sodium chloride aerosol. Since NaCl (and other calibration aerosol salts, e.g. $(NH_4)_2SO_4$) is very hygroscopic, water vapor would meet little resistance during the uptake process and tend to grow as rapidly as possible; a standard of "rapid growth" is obtained, which ambient CCN can be compared against. The size of activated droplets at the exit of the flow chamber depends on the time allowed for growth after activation; given that supersaturation in the instrument requires some length to develop (Lance et al., 2006), particles with low S_c will activate first and grow to larger sizes than particles with S_c equal to the instrument supersaturation. Hence, we choose NaCl particles with S_c equal to the instrument supersaturation (i.e. a dry diameter of D_{p50}), to determine the smallest droplet size, D_{pmin} associated with rapid activation kinetics. Polydisperse ambient aerosol particles entering the CCNc exhibit a range of critical supersaturations, and yield a range of droplet sizes at the exit of the instrument. If activation kinetics is as fast as for the pure salt, the droplet sizes observed in the OPC will thus be equal to (or larger) than the standard for the range of supersaturations measured (Sorooshian et al., 2008; Moore et al., 2008). If the sizes of the droplets formed on ambient aerosol are statistically smaller than the sizes of those formed on pure NaCl aerosol, then the presence of organics likely delay CCN activation; subsequent modeling of growth kinetic data could then express the delay in growth rate in terms of an effective uptake coefficient (e.g. Ruehl et al., 2008; Shantz et al., 2008; Asa-Awuku et al., 2009).

Figure 9 presents application of TDGA to the droplet growth data for the whole measurement period. In agreement with theory (Lance et al., 2006), droplet size augments

as the supersaturation increases. The solid line represents the size of the activated calibration NaCl particles, with S_c equal to the instrument supersaturation, while the points represent the average droplet size from the ambient aerosol activation data. The variability in the droplet size seen in the NaCl data is of the same order as the OPC bin resolution (0.5 μm), and all the ambient droplet size data lie within this uncertainty. Hence, it can be concluded that on average, the aged organics present in ambient aerosol in this area do not significantly delay the CCN activation and growth process. This is consistent with the biogenic SOA studies of Englehart et al. (2008) and Asa-Awuku et al. (2009), where strong kinetic limitations were observed only in situations where the water-soluble fraction of the aerosol was below 30%.

4 Summary and conclusions

Measurements of CCN from 0.21 to 0.73% supersaturation, aerosol size distribution and chemical composition were carried out at the Finokalia measuring site of the University of Crete, during the FAME-07 campaign (September–October, 2007). A variety of airmass types were sampled; polluted air coming from Europe tends to have higher concentrations of smaller particles and contains significant amounts of organic matter. Air masses from Asia Minor and North Africa tend to have lower particle concentrations, with larger CCN sizes and higher activation fraction (CCN/CN). Organics sampled throughout the period were highly oxidized, as about 70% of the total organic mass was found to be water-soluble. Most of the particles activate at 0.6% supersaturation, characteristic of the aged nature of the aerosol sampled.

Application of Köhler theory, using measurements of bulk composition and size distribution resulted in excellent CCN closure. Assuming that organics are insoluble, closure was attained to within 7±11% for all supersaturations, with a tendency for underprediction (16±6%; r^2=0.87) at lowest supersaturation (0.21%). Including the effects of the water-soluble organic fraction reduces the underprediction bias (to 0.6±9%) and the scatter (from R^2=0.9 to 0.92). Therefore, the error associated with application of the simplest form of Köhler theory (i.e. size-invariant composition, and insoluble organic fraction) results in relatively little closure error, notably less in fact than found for other locations close to large anthropogenic sources (e.g. Chang et al., 2007; Ervens et al., 2006; Gunthe et al., 2009; Lance et al., 2009; Medina et al., 2007; Stroud et al. 2007). The maximum level of closure error, seen at low supersaturations (16±10%), when placed in the context of the aerosol indirect effect, results in about a 7±8% uncertainty in cloud droplet number (Sotiropoulou et al., 2006), and if representative of the globe, would result in roughly a 10–15% uncertainty in indirect forcing (Sotiropoulou et al., 2007). Including the effects of water-soluble organics further reduces these uncertainties.

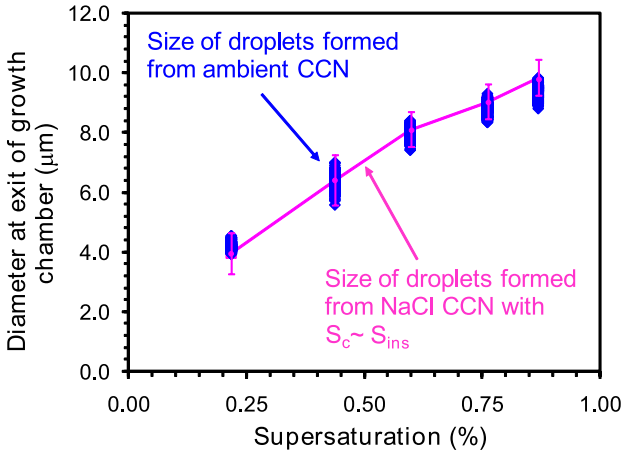

Fig. 9. Droplet sizes of CCN at the different supersaturations for ambient and calibration aerosol.

Using threshold droplet growth analysis, the growth kinetics of ambient CCN is shown to be consistent with NaCl calibration aerosol. This suggests that the presence of aged organics does not seem to suppress the rate of water uptake on ambient CCN. This finding, if applicable to other regions of the globe, would suggest that the CCN activation kinetics of aged aerosol is similar to that of pure inorganic calibration aerosol, hence can be described with one set of kinetic parameters (i.e. uptake coefficient). It should be noted however that all aerosol sampled during FAME-07 was residing in the humid boundary layer before sampling and may contain residual water; whether dry organic-rich particles residing in the free troposphere exhibit different growth kinetic behavior (as suggested by Ruehl et al., 2008) is still unknown and is the objective of a future study.

Acknowledgements. This study is supported by the research project PENED, which is co-financed by EU-European Social Fund (75%) and the Greek Ministry of Development-GSRT (25%). A. Nenes acknowledges support from the US NSF (CAREER) and from NOAA-ACC. S. N. Pandis acknowledges support by NSF-ATM 0732598.

Edited by: A. Wiedensohler

References

Albrecht, B. A.: Aerosols, cloud microphysics, and fractional cloudiness, Science, 245, 1227–1230, 1989.

Asa-Awuku, A., Engelhart, G. J., Lee, B. H., Pandis, S. N., and Nenes, A.: Relating CCN activity, volatility, and droplet growth kinetics of β-caryophyllene secondary organic aerosol, Atmos. Chem. Phys., 9, 795–812, 2009, http://www.atmos-chem-phys.net/9/795/2009/.

Asa-Awuku, A., Sullivan, A. P., Hennigan, C. J., Weber, R. J., and Nenes, A.: Investigation of molar volume and surfactant characteristics of water-soluble organic compounds in biomass burning

aerosol, Atmos. Chem. Phys., 8, 799–812, 2008, http://www.atmos-chem-phys.net/8/799/2008/.

Asa-Awuku, A., Nenes, A., Gao, S., Flagan, R. C., and Seinfeld, J. H.: Alkene ozonolysis SOA: inferences of composition and droplet growth kinetics from Köhler theory analysis, Atmos. Chem. Phys. Discuss., 7, 8983–9011, 2007, http://www.atmos-chem-phys-discuss.net/7/8983/2007/.

Barahona, D. and Nenes, A.: Parameterization of cloud droplet formation in large-scale models: Including effects of entrainment, J. Geophys. Res.-Atmos., 112(D16), D16206, doi:10.1029/2007JD008473, 2007.

Bardouki, H., Liakakou, H., Economou, C., Sciare, J., Smolik, J., Zdimal, V., Eleftheriadis, K., Lazaridis, M., Dye, C., and Mihalopoulos, N.: Chemical composition of size-resolved atmospheric aerosols in the eastern Mediterranean during summer and winter, Atmos. Environ., 37, 195–208, 2003.

Brechtel, F. J. and Kreidenweis, S. M.: Predicting particle critical supersaturation from hygroscopic growth measurements in the humidified TDMA, Part 1: Theory and sensitivity studies, J. Aerosol Sci., 57, 1854–1871, 2000.

Broekhuizen, K., Chang, R.Y.-W., Leaitch, W. R., Li, S.-M., and Abbatt, J. P. D.: Closure between measured and modeled cloud condensation nuclei (CCN) using size-resolved aerosol compositions in downtown Toronto, Atmos. Chem. Phys., 6, 2513–2524, 2006, http://www.atmos-chem-phys.net/6/2513/2006/.

Cantrell, W. G., Shaw, G., Cass, G., Chowdhury, Z., Hughes, L., Prather, K., Guazzotti, S., and Coffee, K.: Closure between aerosol particles and cloud condensation nuclei at Kaashidhoo climate observatory, J. Geophys. Res., 106(D22), 28711–28718, 2001.

Chang, R. Y.-W., Liu, P. S. K., Leaitch, W. R., and Abbatt, J. P. D.: Comparison between measured and predicted CCN concentrations at Egbert, Ontario: Focus on the organic aerosol fraction at a semi-rural site, Atmos. Environ., 41, 8172–8182, 2007.

Charlson, R., Seinfeld, J., Nenes, A., Kulmala, M., Laaksonen, A., and Facchini, M.: Reshaping the theory of cloud formation, Science, 292, 2025–2026, 2001.

Covert, D., Gras, J., Wiedensholer, A., and Stratmann, F.: Comparison of directly measured CCN with CCN modeled from the number-size distribution in the marine boundary layer during ACE 1 at Cape Grim, Tasmania, J. Geophys. Res., 108(D21), 16597–16608, 1998.

Clegg, S. L. and Brimblecombe, P.: Equilibrium partial pressures of strong acids over concentrated saline solutions – I. HNO_3, Atmos. Environ., 22, 91–100, 1988.

CRC, Handbook of Chemistry and Physics, 74th Edition, CRC Press Inc., 1993.

Cross, E. S., Slowik, J. G., Davidovits, P., Allan, J. D., Worsnop, D. R., Jayne, J. T., Lewis, D. K., Canagaratna, M., and Onasch, T. B.: Laboratory and ambient particle density determinations using light scattering in conjunction with aerosol mass spectrometry, Aerosol Sci. Tech., 41, 343–359, 2007.

Decesari, S., Facchini, M. C., Mircea, M., Cavalli, F., and Fuzzi, S.: Solubility properties of surfactants in atmospheric aerosol and cloud/fog water samples, J. Geophys. Res., 108(D21), 4685, doi:10.1029/ 2003JD003566, 2003.

Dinar, E., Taraniuk, I., Graber, E. R., Katsman, S., Moise, T., Anttila, T., Mentel, T. F., and Rudich, Y.: Cloud Condensation Nuclei properties of model and atmospheric HULIS, Atmos. Chem. Phys., 6, 2465–2482, 2006, http://www.atmos-chem-phys.net/6/2465/2006/.

Dusek, U., Covert, D., Wiedensholer, A., Neususs, C., Weise, D., and Cantrell, W.: Cloud condensation nuclei spectra derived from size distributions and hygroscopic properties of the aerosol in coastal southwest Portugal during ACE-2, Tellus, 55B, 35–53, 2003.

Engelhart, G. J., Asa-Awuku, A., Nenes, A., and Pandis, S. N.: CCN activity and droplet growth kinetics of fresh and aged monoterpene secondary organic aerosol, Atmos. Chem. Phys., 8, 3937–3949, 2008, http://www.atmos-chem-phys.net/8/3937/2008/.

Ervens, B., Cubison, M., Andrews, E., Feingold, G., Ogren, J. A., Jimenez, J. L., DeCarlo, P., and Nenes, A.: Prediction of cloud condensation nucleus number concentration using measurements of aerosol size distributions and composition and light scattering enhancement due to humidity, J. Geophys. Res., 112, D10S32, doi:10.1029/2006JD007426, 2007.

Facchini, M., Mircea, M., Fuzzi, S., and Charlson, R.: Cloud albedo enhancement by surface-active organic solutes in growing droplets, Nature, 401, 257–259, 1999.

Finlayson-Pitts, B. J. and Piits Jr., J. N.: Chemistry of the Upper and Lower Atmosphere: Theory, Experiments and Applications, Academic Press, San Diego, California, USA, 2000.

Fountoukis, C. and Nenes, A.: Continued development of a cloud droplet formation parameterization for global climate models, J. Geophys. Res., 110, D11212, doi:10.1029/2004JD005591, 2005.

Furutani, H., Dall'osto, M., Roberts, G. C., and Prather, K. A.: Assessment of the relative importance of atmospheric aging on CCN activity derived from field observations, Atmos. Environ., 42, 3130–3142, 2008.

Gunthe, S. S., King, S. M., Rose, D., Chen, Q., Roldin, P., Farmer, D. K., Jimenez, J. L., Artaxo, P., Andreae, M. O., Martin, S. T., and Pöschl, U.: Cloud condensation nuclei in pristine tropical rainforest air of Amazonia: size-resolved measurements and modeling of atmospheric aerosol composition and CCN activity, Atmos. Chem. Phys. Discuss., 9, 3811–3870, 2009, http://www.atmos-chem-phys-discuss.net/9/3811/2009/.

Hallquist, M., Wenger, J. C., Baltensperger, U., Rudich, Y., Simpson, D., Claeys, M., Dommen, J., Donahue, N. M., George, C., Goldstein, A. H., Hamilton, J. F., Herrmann, H., Hoffmann, T., Iinuma, Y., Jang, M., Jenkin, M. E., Jimenez, J. L., Kiendler-Scharr, A., Maenhaut, W., McFiggans, G., Mentel, T. F., Monod, A., Prévót, A. S. H., Seinfeld, J. H., Surratt, J. D., Szmigielski, R., and Wildt, J.: The formation, properties and impact of secondary organic aerosol: current and emerging issues, Atmos. Chem. Phys., 9, 5155–5235, 2009, http://www.atmos-chem-phys.net/9/5155/2009/.

Intergovernmental Panel on Climate Change: Climate Change 2007: Synthesis Report, 2007.

Jaffrezo, J.-L., Aymoz, G., Delaval, C., and Cozic, J.: Seasonal variations of the water soluble organic carbon mass fraction of aerosol in two valleys of the French Alps, Atmos. Chem. Phys., 5, 2809–2821, 2005, http://www.atmos-chem-phys.net/5/2809/2005/.

Ji, Q., Shaw, G., and Cantrell, W.: A new instrument for measuring cloud condensation nuclei: Cloud condensation nucleus "remover", J. Geophys. Res., 103, 28013–28019, 1998.

Köhler, H.: Zur condensation des wasserdampfe in der atmosphere, Geofys. Publ., 2, 3–15, 1921.

Köhler, H.: The nucleus in the growth of hygroscopic droplets, T. Faraday Soc., 32, 1152, 1936.

Kostenidou, E., Pathak, R. K., and Pandis, S.: An algorithm for the calculation of secondary organic aerosol density combining AMS and SMPS data, Aerosol Sci. Tech., 41(11), 1002–1010, 2007.

Koulouri, E., Saarikoski, S., Theodosi, C., Markaki, Z., Gerasopoulos, E., Kouvarakis, G., Mäkelä, T., Hillamo, R., and Mihalopoulos, N.: Chemical composition and sources of fine and coarse particles in the Eastern Mediterranean, Atmos. Environ., 42, 6542–6550, 2008.

Krämer, L., Pöschl, U., and Niessner, R.: Microstructural rearrangement of sodium chloride condensation aerosol particles on interaction with water vapor, J. Aerosol Sci., 31, 673–685, 2000.

Lance, S., Medina, J., Smith, J., and Nenes, A.: Mapping the operation of the DMT continuous flow CCN counter, Aerosol Sci. Tech., 40, 242–254, 2006.

Lance, S., Nenes, A., Mazzoleni, C., Dubey, M. K., Gates, H., Varutbangkul, V., Rissman, T. A., Murphy, S. M., Sorooshian, A., Flagan, T. A., Seinfeld, J. H., Feingold, G., and Jinsson, H.: Cloud condensation nuclei activity, closure, and droplet growth kinetics of Houston aerosol during the Gulf of Mexico Atmospheric Composition and Climate Study (GoMACCS), J. Geophys. Res., 114, D00F15, doi:10.1029/2008JD011699, 2009.

Lelieveld, J., Berresheim, H., Borrmann, S., Crutzen, P. J., Dentener, F. J., Fischer, H., Feichter, J., Flatau, P. J., Heland, J., Holzinger, R., Korrmann, R., Lawrence, M. G., Levin, Z., Markowicz, K. M., Mihalopoulos, N., Minikin, A., Ramanathan, V., De Reus, M., Roelofs, G. J., Scheeren, H. A., Sciare, J., Schlager, H., Schultz, M., Siegmund, P., Steil, B., Stephanou, E. G., Stier, P., Traub, M., Warneke, C., Williams, J., and Ziereis, H.: Global Air Pollution Crossroads over the Mediterranean, Science, 298, 794–799, 2002.

Liu, P., Leaitch, W., Banic, C., Li, S., Ngo, D., and Megaw, W.: Aerosol observations at Chebogue Point during the 1993 North Atlantic Regional Experiment: Relationships among cloud condnensation nuclei, size distribution and chemistry, J. Geophys. Res., 101, 28971–28990, 1996.

Maenhaut, W., Hillamo, R., Mäkelä, T., Jafferzo, J.-L., Bergin, M. H., and Davidson, C. I.: A new cascade impactor for aerosol sampling with subsequent PIXE analysis, Nucl. Instr. Meth. B, 109/110, 482–487, 1996.

McMurry, P. H., Wang, X., Park, K., and Ehara, K.: The relationship between mass and mobility for atmospheric particles: A new technique for measuring particle density, Aerosol Sci. Tech., 36, 227–238, 2002.

Medina, J., Nenes, A., Sotiropoulou, R.-E. P., Cottrell, L. D., Ziemba, L. D., Beckman, P. J., and Griffin, R. J.: Cloud condensation nuclei closure during the International Consortium for Atmospheric Research on Transport and Transformation 2004 campaign: Effects of size-resolved composition, J. Geophys. Res., 112, D10S31, doi:10.1029/2006JD007588, 2007.

Mihalopoulos, N., Stephanou, E., Kanakidou, M., Pilitsidis, S., and Bousquet, P.: Tropospheric aerosol ionic composition above the Eastern Mediterranean area, Tellus, 49B, 314–326, 1997.

Mikhailov, E., Vlasenko, S., Niessner, R., and Pöschl, U.: Interaction of aerosol particles composed of protein and saltswith water vapor: hygroscopic growth and microstructural rearrangement, Atmos. Chem. Phys., 4, 323–350, 2004, http://www.atmos-chem-phys.net/4/323/2004/.

Mircea, M., Facchini, M. C., Decesari, S., Cavalli, F., Emblico, L., Fuzzi, S., Vestin, A., Rissler, J., Swietlicki, E., Frank, G., Andreae, M. O., Maenhaut, W., Rudich, Y., and Artaxo, P.: Importance of the organic aerosol fraction for modeling aerosol hygroscopic growth and activation: a case study in the Amazon Basin, Atmos. Chem. Phys. Discuss., 5, 5253–5298, 2005, http://www.atmos-chem-phys-discuss.net/5/5253/2005/.

Moore, R. H., Ingall, E. D., Sorooshian, A., and Nenes, A.: Molar mass surface tension, and droplet growth kinetics on marine organics from measurements of CCN activity, Geophys. Res. Lett., 35, L07801, doi:10.1029/2008GL033350, 2008.

Murphy, S. M., Agrawal, H., Sorooshian, A., Padro, L. T., Gates, H., Hersey, S., Welch, W. A., Jung, H., Miller, J. W., Cocker III, D. R., Nenes, A., Jonsson, H. H., Flagan, R. C., and Seinfeld, J. H.: Comprehensive Simultaneous Shipboard and Airborne Characterization of Exhaust from a Modern Container Ship at Sea, Environ. Sci. Technol., 43, 13, 4626–4640, 2009.

Nenes, A., Ghan, S., Abdul-Razzak, H., Chuang, P., and Seinfeld, J. H.: Kinetic limitations on cloud droplet formation and impact on cloud albedo, Tellus, 53B, 133–149, 2001.

Nenes, A., Charlson, R. J., Facchini, M. C., Kulmala, M., Laaksonen, A., and Seinfeld, J. H.: Can chemical effects on cloud droplet number rival the first indirect effect?, Geophys. Res. Lett., 29(17), 1848, doi:10.1029/2002GL015295, 2002.

Padró, L. T., Asa-Awuku, A., Morrison, R., and Nenes, A.: Inferring thermodynamic properties from CCN activation experiments: single-component and binary aerosols, Atmos. Chem. Phys., 7, 5263–5274, 2007, http://www.atmos-chem-phys.net/7/5263/2007/.

Petters, M. D. and Kreidenweis, S. M.: A single parameter representation of hygroscopic growth and cloud condensation nucleus activity, Atmos. Chem. Phys., 7, 1961–1971, 2007, http://www.atmos-chem-phys.net/7/1961/2007/.

Pitzer, K. S.: Thermodynamics of electrolytes, I, Theoretical Basis and general equations, J. Phys. Chem., 77, 268–277, 1973.

Pitzer, K. S. and Mayorga, G.: Thermodynamics of electrolytes, II, Activity and osmotic coefficients for strong electrolytes with one or both ions univalent, J. Phys. Chem., 77, 2300–2308, 1973.

Reade, L., Jennings, S. G., and McSweeney, G.: Cloud condensation nuclei measurements at Mace Head, Ireland, over a period 1994–2002, Atmos. Res., 82, 610–621, 2006.

Rissman, T. A., VanReken, T. M., Wang, J., Gasparini, R., Collins, D. R., Jonsson, H. H., Brechtel, F. J., Flagan, R. C., and Seinfeld, J. H.: Characterization of ambient aerosol from measurements of cloud condensation nuclei during the 2003 atmospheric radiation measurement aerosol intensive observational period at the Southern Great Plains site in Oklahoma, J. Geophys. Res., 111, D05S11/1–D05S11/20, 2006.

Roberts, G. C., Nenes, A., Seinfeld, J. H., and Andreae, M. O.: Impact of biomass burning on cloud properties in the Amazon Basin, J. Geophys. Res, 108(D2), 4062, doi:10.1029/2001JD000985, 2003.

Roberts, G. and Nenes, A.: A continuous-flow streamwise thermal-gradient CCN chamber for atmospheric measurements, Aerosol Sci. Tech., 39, 206–221, 2005.

Roberts, G. C., Mauger, G., Hadley, O., and Ramanathan, V.: North

American and Asian aerosols over the Eastern Pacific Ocean and their role in regulating cloud condensation nuclei, J. Geophys. Res., 111, D13205, doi:10.1029/2005JD006661, 2006.

Rose, D., Nowak, A., Achtert, P., Wiedensohler, A., Hu, M., Shao, M., Zhang, Y., Andreae, M. O., and Pöschl, U.: Cloud condensation nuclei in polluted air and biomass burning smoke near the mega-city Guangzhou, China - Part 1: Size-resolved measurements and implications for the modeling of aerosol particle hygroscopicity and CCN activity, Atmos. Chem. Phys. Discuss., 8, 17343–17392, 2008,
http://www.atmos-chem-phys-discuss.net/8/17343/2008/.

Rose, D., Gunthe, S. S., Mikhailov, E., Frank, G. P., Dusek, U., Andreae, M. O., and Pöschl, U.: Calibration and measurement uncertainties of a continuous-flow cloud condensation nuclei counter (DMT-CCNC): CCN activation of ammonium sulfate and sodium chloride aerosol particles in theory and experiment, Atmos. Chem. Phys., 8, 1153–1179, 2008,
http://www.atmos-chem-phys.net/8/1153/2008/.

Ruehl, C. R., Chuang, P. Y., and Nenes, A.: How quickly do cloud droplets form on atmospheric particles?, Atmos. Chem. Phys., 8, 1043–1055, 2008,
http://www.atmos-chem-phys.net/8/1043/2008/.

Salma, I., Ocskay, R., Varga, I., and Maenhaut, W.: Surface tension of atmospheric humic-like substances in connection with relaxation, dilution and solution pH, J. Geophys. Res., 111, D23205, doi:10.1029/2005JD007015, 2006.

Seinfeld, J., and Pandis, S.: Atmospheric Chemistry and Physics: From Air Pollution to Climate Change, John Wiley, Hoboken, N. J., 1998.

Sciare, J., Oikonomou, K., Cachier, H., Mihalopoulos, N., Andreae, M. O., Maenhaut, W., and Sarda-Estève, R.: Aerosol mass closure and reconstruction of the light scattering coefficient over the Eastern Mediterranean Sea during the MINOS campaign, Atmos. Chem. Phys., 5, 2253–2265, 2005,
http://www.atmos-chem-phys.net/5/2253/2005/.

Shantz, N. C., Leaitch, W. R., Phinney, L., Mozurkewich, M., and Toom-Sauntry, D.: The effect of organic compounds on the growth rate of cloud droplets in marine and forest settings, Atmos. Chem. Phys., 8, 5869–5887, 2008,
http://www.atmos-chem-phys.net/8/5869/2008/.

Shulman, M., Jacobson, M., Charlson, R., Synovec, R., and Young, T.: Dissolution behavior and surface tension effects of organic compounds in nucleating cloud droplets, Geophys. Res. Lett., 23, 277–280, 1996.

Snider, J., Guibert, S., Brenguier, J., and Putaud, J.: Aerosol activation in marine stratocumulus clouds: 2, Köhler and parcel theory closures studies, J. Geophys. Res., 108(D15), 8629, doi:10.1029/2002JD002692, 2003.

Sorooshian, A., Murphy, S. M., Hersey, S., Gates, H., Padro, L. T., Nenes, A., Brechtel, F. J., Jonsson, H., Flagan, R. C., and Seinfeld, J. H.: Comprehensive airborne characterization of aerosol from a major bovine source, Atmos. Chem. Phys., 8, 5489–5520, 2008,
http://www.atmos-chem-phys.net/8/5489/2008/.

Sotiropoulou, R. E. P, Nenes, A., Adams, P. J., and Seinfeld, J. H.: Cloud condensation nuclei prediction error from application of Kohler theory: Importance for the aerosol indirect effect, J. Geoph. Res., 112, D12202, doi:10.1029/2006JD007834, 2007.

Sotiropoulou, R. E. P, Medina, J., and Nenes, A.: CCN predictions: is theory sufficient for assessments of the indirect effect?, Geophs. Res. Lett., 33, L05816, doi:10.1029/2005GL025148, 2006.

Stein, S. W., Turpin, B. J., Cai, X., Huang, P.-F., and McMurry, P. H.: Measurements of relative humidity-dependent bounce and density for atmospheric particles using the DMA-impactor technique, Atmos. Environ., 28, 1739–1746, 1994.

Stroud, C. A., Nenes, A., Jimenez, J. L., DeCarlo, P. F., Huffman, J. A., Bruintjes, R., Nemitz, E., Delia, A. E., Toohey, D. W., Guenther, A. B., and Nandi, S.: Cloud activating properties of aerosol observed during CELTIC, J. Atmos. Sci., 64, 441–459, 2006.

Turšiè, J., Podkrajšek, B., Grgić, I., Ctyroky, P., Berner, A., Dusek, U., and Hitzenberger, R.: Chemical composition and hygroscopic properties of size-segregated aerosol particles collected at the Adriatic coast of Slovenia, Chemosphere, 63, 1193–1202, 2006.

Twomey, S.: The influence of pollution on the shortwave albedo of clouds, J. Atmos. Sci., 34, 1149–1152, 1977.

VanReken, T. M., Rissman, T. A., Roberts, G. C., Varutbangkul, V., Jonsson, H. H., Flagan, R. C., and Seinfeld, J. H.: Toward aerosol/cloud condensation nuclei (CCN) closure during CRYSTAL-FACE, J. Geophys. Res., 108(D20), 4633, doi:10.1029/2003JD003582, 2003.

Vrekoussis, M., Liakakou, E., Koçak, M., Kubilay, N., Oikonomou, K., Sciare, J., and Mihalopoulos, N.: Seasonal variability of optical properties of aerosols in the Eastern Mediterranean, Atmos. Environ., 39, 37, 7083–7094, 2005.

Ziese, M., Wex, H., Nilsson, E., Salma, I., Ocskay, R., Hennig, T., Massling, A., and Stratmann, F.: Hygroscopic growth and activation of HULIS particles: experimental data and a new iterative parameterization scheme for complex aerosol particles, Atmos. Chem. Phys., 8, 1855–1866, 2008,
http://www.atmos-chem-phys.net/8/1855/2008/.